

DOI: 10.1002/cmdc.201000449

Potent and Selective Inhibition of Cysteine Proteases from *Plasmodium falciparum* and *Trypanosoma brucei*

Veronika Ehmke,^[a] Cornelia Heindl,^[b] Matthias Rottmann,^[c, d] Céline Freymond,^[c, d] W. Bernd Schweizer,^[a] Reto Brun,^[c, d] August Stich,^[e] Tanja Schirmeister,^[b] and François Diederich^{*[a]}

Malaria and African sleeping sickness (human African trypanosomiasis), caused by the parasitic protozoa *Plasmodium falciparum* and *Trypanosoma brucei*, respectively, are among the most severe tropical diseases and represent major health issues in the developing world.^[1,2] Approximately 250 million malaria infections and 1 million deaths are registered annually, with up to 70% of the clinical cases attributed to *P. falciparum* concentrated within the African region.^[1,3] Human African trypanosomiasis threatens millions of people in about 20 sub-Saharan countries in Africa, with an estimated annual number of cases between 50 000 and 70 000 and an annual mortality close to 25 000.^[4] The emergence of multidrug-resistant parasite strains, in addition to limited available chemotherapies, demand the urgent development of new and effective drugs with novel mechanisms of actions. *P. falciparum* and *T. brucei* offer several potential target enzymes that are implicated in pathogenesis and host cell invasion, including a number of essential and closely related cysteine proteases.^[5] The largest subfamily among them are the papain-like cysteine proteases (clan CA, family C1).

In *P. falciparum*, various proteases catalyze the degradation of human hemoglobin to provide nutrients for exponential growth and maturation of the pathogen.^[6] Hemoglobin catabolism is initiated by a series of aspartic proteases, the plasmepsins, and a histidine-aspartic protease to perform the first proteolytic cleavage. Further degradation into smaller peptidic fragments is achieved by unique food–vacuole cysteine proteases, the falcipains.^[7] Biological studies revealed overlapping activity profiles of plasmepsins and falcipains, and it was further concluded that plasmepsins are processed and activated by falcipains.^[8,9] This catabolic process is both vital and specific for parasitic survival. Inhibition of falcipains has proven indis-

pensable in order to completely block parasitic growth and proliferation.^[10] Falcipain-2, -2', and -3 are the key hemoglobinases of the erythrocytic parasite.^[11] Falcipain-2, the most abundant and best-studied of these enzymes, has emerged as a promising target for the development of novel drugs.^[10,12]

Bloodstream *T. brucei rhodesiense* parasites express the cysteine protease rhodesain, a cathepsin L-like hydrolase. Rhodesain is involved in the degradation of parasitic and intracellularly transported host proteins, and is responsible for general proteolytic activity in all life stages of the organism.^[13,14] Cysteine protease inhibitors have been shown to kill African trypanosomes in vitro and in animal models.^[15]

Various types of falcipain-2 and rhodesain inhibitors have been developed in the last years, mainly based on screening methods.^[16,17] However, we felt our expertise in structure-based design would enable us to obtain new potent and selective inhibitors without the need for screening.^[18] We began our investigations based on the first X-ray crystal structures of falcipain-2, available since 2006 (Protein Data Bank (PDB) codes: 1YVB, 2GHU, 3BPF),^[19–21] and of rhodesain published only recently in 2009 and 2010 (PDB codes: 2P7U, 2P86).^[22,23] Both falcipain-2 and rhodesain share the common features of clan CA cysteine proteases with the classical papain fold consisting of two distinct domains. Superimposition of the structures of both enzymes reveals a high degree of analogy in their overall fold, with highest conservation observed for the catalytic domain (Figure 1 a). Sequence alignment of the catalytic domains resulted in the assignment of both enzymes to the cathepsin L-like subfamily.^[17] In both structures, the catalytic dyad (falcipain-2: Cys 42, His 174; rhodesain: Cys 25, His 162) is embedded in a channel-like junction between the two domains with a highly conserved peptide sequence (Figure 1 b). The active site extends further into the apolar S2 pocket with a strong preference for hydrophobic substituents.^[10,12] Previous work suggested that the S2 pocket is the key determinant of substrate specificity in papain-like cysteine proteases.^[24]

The general structure of cysteine protease inhibitors contains prevalently an electrophilic moiety to form a reversible, covalent thioimidate intermediate with the catalytic cysteine. We opted, specifically, for inhibitors featuring a nitrile residue as the electrophilic head group. More than 30 nitrile-containing pharmaceuticals are prescribed for a variety of medicinal indications, and several are in clinical development.^[25,26] Unsurprisingly, nitriles are a well established class of cysteine protease inhibitors.^[27,28] Oballa et al. hypothesized that the increased electrophilicity of the nitrile moiety could impact the reversibility of enzyme–inhibitor complex formation.^[29] According to their calculated reactivities, aryl nitriles, particularly pyri-

[a] V. Ehmke, Dr. W. B. Schweizer, Prof. Dr. F. Diederich
Laboratory of Organic Chemistry, ETH Zürich
Wolfgang-Pauli-Strasse 10, 8093 Zürich (Switzerland)
Fax: (+41)44-632-1109
E-mail: diederich@org.chem.ethz.ch

[b] C. Heindl, Prof. Dr. T. Schirmeister
Institute of Pharmacy and Food Chemistry, University of Würzburg
Am Hubland, 97074 Würzburg (Germany)

[c] Dr. M. Rottmann, C. Freymond, Prof. Dr. R. Brun
Swiss Tropical and Public Health Institute
Socinstrasse 57, 4002 Basel (Switzerland)

[d] Dr. M. Rottmann, C. Freymond, Prof. Dr. R. Brun
University of Basel, Petersplatz 1, 4003 Basel (Switzerland)

[e] Dr. A. Stich
Department of Tropical Medicine, Medical Mission Institute
Salvatorstrasse 7, 97074 Würzburg (Germany)

Supporting information for this article is available on the WWW under <http://dx.doi.org/10.1002/cmdc.201000449>.

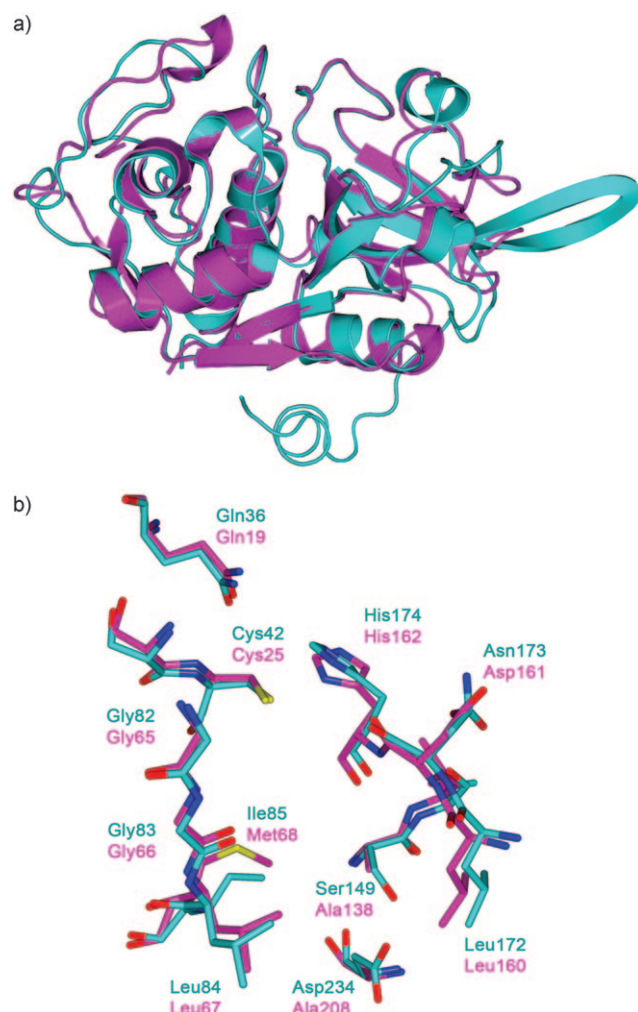


Figure 1. a) Superimposition of X-ray crystal structures of falcipain-2 (cyan, PDB code: 2GHU) and rhodesain (magenta, PDB code: 2P86); b) Superimposition of selected amino acids in the active site of falcipain-2 (C skeleton: cyan) and rhodesain (C skeleton: magenta). Color code: O atoms: red, N atoms: blue, S atoms: yellow.

midine and triazine nitriles, should possess the most reactive nitrile moieties.

Herein, we describe the structure-based design, efficient synthesis, and biological evaluation of a new series of triazine nitrile inhibitors to explore the binding properties of falcipain-2 and rhodesain. Guided by molecular modeling, we propose a binding model showing the accommodation of the different vectors in the apolar pockets of the active site. The inhibitors were tested against closely related human and viral cysteine proteases, as well as a serine protease, to investigate their general selectivity. Additionally, *in vitro* activity against *P. falciparum* and *T. brucei rhodesiense* parasites and cytotoxicity was studied.

Computer-aided modeling using the MAB force field within MOLOC^[30] was applied to design small drug-like molecules to occupy the active site. We identified a diamino-substituted triazine as suitable central scaffold to position vectors for the S1, S2, and S3 binding pockets and direct the thioimidate adduct into the stabilizing oxyanion hole (Figure 2a). Occupancy of

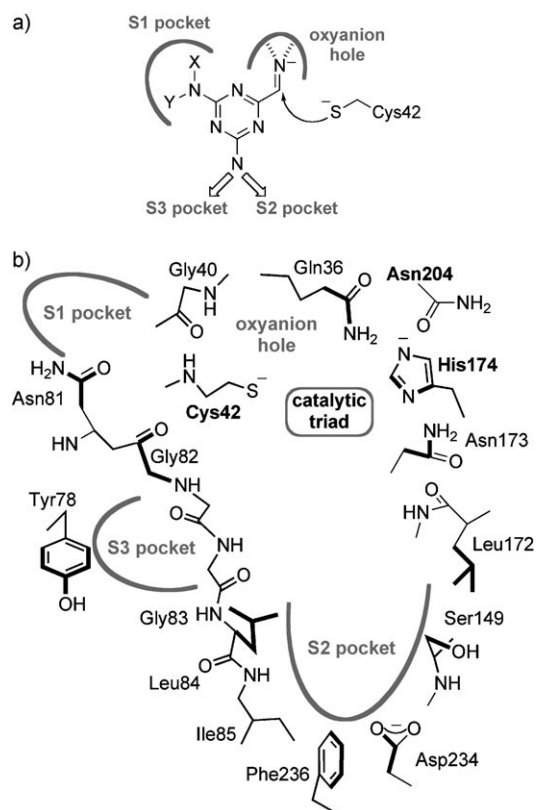


Figure 2. a) Schematic representation of the triazine nitrile core, stabilization of the thioimidate in the oxyanion hole, and positioning of the vectors; b) Simplified diagram of the active site of falcipain-2 showing the catalytic dyad, the oxyanion hole, and the S1, S2, and S3 pockets.

the various pockets (Figure 2b) was subsequently optimized to gain high binding potency.

Active site analysis and 3D modeling revealed that a morpholine residue could act as suitable substituent to address the flat, predominantly solvent-exposed S1 pocket in falcipain-2. For occupancy of the large and mainly hydrophobic S2 pocket, we identified a 4-(*n*-propyl)cyclohexyl substituent as optimal vector, undergoing several hydrophobic interactions with the side chains of Leu84, Ile85, and Ser149. To reach the wide S3 pocket, a 1,3-benzodioxol-5-yl moiety was chosen to stack on the amide backbone of Gly82 and Gly83. Figure 3 shows the proposed binding mode for lead compound **1** in the active site of falcipain-2.

We prepared a series of functionalized triazine nitrile inhibitors by varying the S1, S2, and S3 substituents. The synthesis of inhibitor **1** is shown in Scheme 1. Reductive amination of ketone **2** and amine **3** gave secondary amine **4** in good yield. Amine **4** was subsequently transformed into 4,6-dichlorotriazine derivative **5** by reaction with equimolar amounts of cyanuric chloride (2,4,6-trichloro-1,3,5-triazine) and *N,N*-diisopropylethylamine (*i*Pr₂NEt) at 0 °C. Introduction of the second vector was achieved by subsequent nucleophilic aromatic substitution with morpholine under basic conditions to give **6**. Cyanation of **6** using potassium cyanide in dimethyl sulfoxide at high temperature afforded ligand **1**. Compounds **7–17** were accessed by similar routes. In addition, an efficient

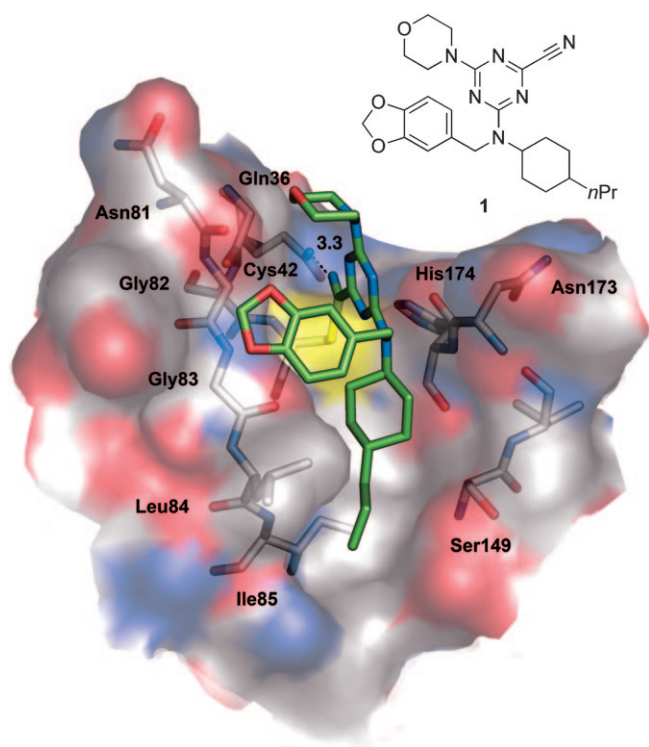
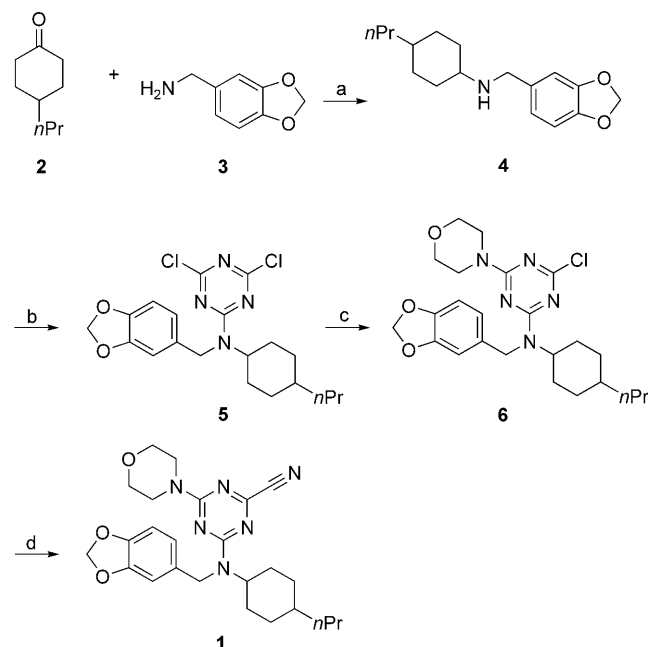


Figure 3. Binding mode of inhibitor **1** in the active site of falcipain-2 (PDB code: 2GHU) as proposed by docking and energy minimization using MOLOC. Color code: C skeleton of enzyme: grey, C skeleton of **1**: green, O atoms: red, N atoms: blue, S atom: yellow. H-bond distance is given in Å.



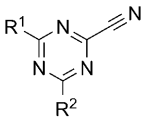
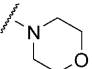
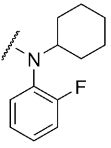
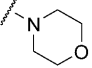
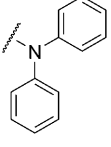
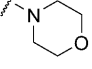
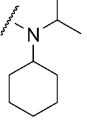
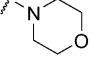
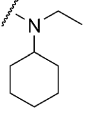
Scheme 1. Synthesis of inhibitor **1**. a) 1) CH_2Cl_2 , molecular sieves (4 Å), 25°C , 1.5 h, 2) $\text{NaBH}(\text{OAc})_3$, 25°C , 15 h, 71%; b) cyanuric chloride, $i\text{Pr}_2\text{NEt}$, CH_2Cl_2 , 0°C , 4 h, 79%; c) morpholine, $i\text{Pr}_2\text{NEt}$, CH_2Cl_2 , $0^\circ\text{C} \rightarrow 25^\circ\text{C}$, 3.5 h, 84%; d) KCN, Me_2SO , 120°C , 4.5 h, 27%.

one-pot procedure for the two nucleophilic chlorine substitution steps was developed for compounds **13**, **14**, **16**, and **17** (for detailed experimental procedures, see the Supporting Information). Single crystals, suitable for X-ray analysis, were obtained for inhibitors **7**, **13**, and **15**^[31] (figures 1SI–3SI in the Supporting Information) confirming the constitution and favorable structural organization of the 4,6-diamino-1,3,5-triazine-2-carbonitrile compounds.

All compounds were tested against falcipain-2 from *P. falciparum* and rhodesain from *T. brucei rhodesiense* (Table 1), respectively, in standard fluorescence-based assays (see the Supporting Information).^[32,33] For falcipain-2, investigation of substituents for the mostly solvent-exposed S1 pocket revealed a

Table 1. Inhibition of falcipain-2 and rhodesain by compounds **1** and **7–17**.^[a]

Compd	R ¹	R ²	K _i [nM]	
			falcipain-2	rhodesain
1 ^[b]			1030 ± 120	2 ± 1
7 ^[b]			35 ± 3	490 ± 190
8			n.d. ^[c]	970 ± 200
9 ^[b]			20 ± 7	8 ± 1
10			n.d.	n.d.
11 ^[d]			12900 ± 100	n.d.
12 ^[d]			9800 ± 500	n.d.
13 ^[b]			36 ± 7	34 ± 3

Table 1. (Continued)					
Compd	R ¹	R ²		K _i [nM]	
				falcipain-2	rhodesain
14 ^[b]				25 ± 5	11 ± 1
15 ^[b]				42 ± 7	36 ± 7
16 ^[b]				29 ± 5	74 ± 2
17 ^[b]				80 ± 1	100 ± 40

[a] All results are the mean of at least two independent measurements, each performed in duplicate. [b] Time-dependent inhibition. [c] n.d. = not determined; less than 35% inhibition in initial screen at 20 μM. [d] ad = 2-adamantyl.

preference for the initially designed morpholine group, whereas cyclopropylamine derivative **8** proved to be inactive. Replacement of the morpholine with a 2-methoxyethylamine vector resulted in no significant change in inhibitory constants (**11**: $K_i = 12900 \pm 100$ nM; **12**: $K_i = 9800 \pm 500$ nM). The affinity of initially designed active compound **1** ($K_i = 1030 \pm 120$ nM) was considerably enhanced by omitting the *n*-propyl substituent. Compound **9**, with an unsubstituted cyclohexyl moiety, was significantly more potent against falcipain-2 ($K_i = 20 \pm 7$ nM). Introduction of a bulkier 2-adamantyl group resulted in a loss of affinity by three orders of magnitude (**11**: $K_i = 12900 \pm 100$ nM) > 4-(*n*-propyl)cyclohexyl (**1**: $K_i = 1030 \pm 120$ nM) > cyclohexyl (**9**: $K_i = 20 \pm 7$ nM). Furthermore, a phenyl ring was also found to be a suitable substituent for the S2 pocket: phenyl-substituted ligands yielded activities in the low nanomolar range (**13**: $K_i = 36 \pm 7$ nM; **14**: $K_i = 25 \pm 5$ nM; **15**: $K_i = 42 \pm 7$ nM). These data emphasize the importance of proper occupancy of the S2 pocket, as previously reported.^[28] Variation of substituents for the wide S3 pocket revealed a preference for 1,3-benzodioxol-5-yl and cyclohexyl substituents (**7**: $K_i = 35 \pm 3$ nM; **9**: $K_i = 20 \pm 7$ nM). Replacement of the 1,3-benzodioxol-5-yl moiety with a 3-(trifluoromethyl)benzyl residue resulted in complete loss of ac-

tivity for compound **10**. Introduction of smaller ethyl or isopropyl substituents again led to inhibitory constants in the double-digit nanomolar range (**16**: $K_i = 29 \pm 5$ nM; **17**: $K_i = 80 \pm 1$ nM).

Inhibitory constants for the compounds were also assessed against rhodesain from *T. brucei rhodesiense*. Lead compound **1** and unsubstituted cyclohexyl analogue **9** exhibited the highest affinities in this series, with K_i values of 2 ± 1 nM and 8 ± 1 nM, respectively. In general, activities against falcipain-2 and rhodesain correlate well; however, notable differences were observed regarding the occupancy of the S2 pocket. The 2-adamantyl-substituted triazines **11** and **12** were moderately active against falcipain-2 but inactive against rhodesain, suggesting a less extended S2 pocket within the latter enzyme. Most importantly, the two enzymes differ at the bottom of this pocket; while falcipain-2 has a strong preference for a shorter cyclohexyl substituent (**9**: $K_i = 20 \pm 7$ nM) over 4-(*n*-propyl)cyclohexyl (**1**: $K_i = 1030 \pm 120$ nM), both **1** and **9** display K_i values against rhodesain in the single-digit nanomolar range (**1**: $K_i = 2 \pm 1$ nM; **9**: 8 ± 1 nM). Modeling suggests that the bottom of the pocket in falcipain-2, lined by Ile 85 and Asp 234, is narrower and more polar than the comparable region in rhodesain, lined by Met 68 and Ala 208 (see figures 4SI and 5SI in the Supporting Information).

Competitive inhibition was confirmed by determination of apparent dissociation constants for rhodesain inhibition by compound **1** at various substrate concentrations, revealing a linear relationship between apparent dissociation constant and substrate concentration.^[34] These results can presumably be assigned to the whole series.

In order to study the general selectivity of the synthesized inhibitors against related cysteine proteases, the compounds were tested against human cathepsin B and cathepsin L,^[17] and against the severe acute respiratory syndrome–coronavirus (SARS-CoV) papain-like protease and main protease (table 1SI in the Supporting Information).^[35] Superimposition of selected amino acids in the active sites of falcipain-2, cathepsin B, and cathepsin L emphasizes their structural similarity (see figure S6 in the Supporting Information). Only compounds **9**, **14**, **15**, and **17** showed affinity for human cathepsin L in the low nanomolar range, whereas moderate to good selectivity against this enzyme was observed for derivatives **1**, **7**, **11**, **12**, **13**, **16**, and **17**. Moreover, all compounds were highly selective against human cathepsin B and the viral cysteine proteases. Furthermore, all compounds were inactive against α -chymotrypsin,^[35] revealing selectivity for cysteine over serine proteases.

The newly synthesized compounds were tested for their ability to inhibit growth of the malaria parasite *P. falciparum* and the trypanosomatid *T. brucei rhodesiense* in vitro (Table 2). Nitriles **1**, **7**, **9**, **10**, **11**, **12**, and **16** exhibited moderate activities against *P. falciparum* with IC₅₀ values between 0.6 and 3.7 μM. IC₅₀ values against *T. brucei rhodesiense* trypomastigotes ranged from 15.0 μM to 44.1 μM. Comparable data were obtained from assays against *T. brucei brucei* (strain TC221; data not shown). A correlation between inhibition of the parasitic cysteine proteases and in vitro activity could not be established. This might be due to off-target effects, physical chemical prop-

Table 2. In vitro activities of compounds 1 and 7–17 against *P. falciparum* and *T. brucei rhodesiense*.^[a]

Compd	IC ₅₀ [μM]		
	<i>P. falciparum</i> ^[b]	<i>T. b. rhodesiense</i> ^[c]	L-6 cells ^[d]
1	2.4	31.2	5.9
7	3.7	31.9	25.1
8	> 5.0	25.8	23.5
9	2.9	30.1	11.1
10	0.6	34.2	4.5
11	1.1	27.5	23.2
12	1.8	19.6	8.1
13	> 5.0	16.7	17.9
14	> 5.0	15.0	11.4
15	> 5.0	18.9	22.0
16	3.4	30.9	25.9
17	> 5.0	44.1	45.5

[a] All results are the mean of at least two independent measurements, each performed in duplicate. [b] *P. falciparum* strain NF54. [c] *T. brucei rhodesiense* strain STIB 900, trypomastigote stage. [d] Rat skeletal myoblasts were used to assess cytotoxicity.

erties of the compounds, or general cytotoxic effects, as indicated by cytotoxicity observed against L-6 rat myoblast cells (Table 2) and human macrophages (data not shown), leading to low selectivity indices. Investigations are currently ongoing to improve in vitro selectivity of the compounds.

In conclusion, we designed and synthesized a small library of potent and selective competitive inhibitors of the protozoan cysteine proteases falcipain-2 and rhodesain. Promising inhibitory activities down to $K_i = 20 \pm 7$ nM for falcipain-2 and $K_i = 2 \pm 1$ nM for rhodesain were obtained for these first generation triazine nitrile-based ligands. A major difference between the two closely related enzymes was observed in the optimal occupation of the S2 pocket, which appears to be narrower and more polar in falcipain-2 as compared to rhodesain. Biological assays showed, in some cases, good selectivity against closely related human cathepsin L, and overall high selectivity against cathepsin B, viral cysteine proteases, and α -chymotrypsin. In contrast to excellent enzymatic activity and good selectivity, in vitro studies revealed moderate activity for the majority of synthesized compounds against *P. falciparum* and marginal activity against *T. brucei rhodesiense*. Further studies are necessary to explore to what extent the inhibitors reach their actual biological targets in order to understand their low activity in the cell-based assays.

Acknowledgements

V.E. is grateful for a Kekulé fellowship from the German Fonds der Chemischen Industrie. Financial support by the Deutsche Forschungsgemeinschaft (DFG, SFB 630, TPA4 to T.S.) and the Swiss National Science Foundation is gratefully acknowledged. We thank Jennifer Rath and Svetlana Sologub for performing the Trypanosoma brucei brucei and macrophages assays, Dr. Daniel Bur (Actelion Pharmaceuticals Ltd.) for helpful discussions, and Dr. Valentina Aureggi and Laura Salonen for reviewing the manuscript.

Keywords: African trypanosomiasis • cysteine proteases • inhibitors • malaria • structure-based design

- [1] R. W. Snow, C. A. Guerra, A. M. Noor, H. Y. Myint, S. I. Hay, *Nature* **2005**, *434*, 214–217.
- [2] J. M. Sternberg, *Parasite Immunol.* **2004**, *26*, 469–476.
- [3] World Health Organisation (WHO), *Malaria*, fact sheet N°94, **2010**; www.who.int/mediacentre/factsheets/fs094/en/.
- [4] R. Brun, J. Blum, F. Chappuis, C. Burri, *Lancet* **2010**, *375*, 148–159.
- [5] J. H. McKerrow, E. Sun, P. J. Rosenthal, J. Bouvier, *Annu. Rev. Microbiol.* **1993**, *47*, 821–853.
- [6] L. H. Miller, D. I. Baruch, K. Marsh, O. K. Doumbo, *Nature* **2002**, *415*, 673–679.
- [7] G. H. Coombs, D. E. Goldberg, M. Klemba, C. Berry, J. Kay, J. C. Mottram, *Trends Parasitol.* **2001**, *17*, 532–537.
- [8] A. L. Omara-Opyene, P. A. Moura, C. R. Sulsona, J. A. Bonilla, C. A. Yowell, H. Fujioka, D. A. Fidock, J. B. Dame, *J. Biol. Chem.* **2004**, *279*, 54088–54096.
- [9] M. E. Drew, R. Banerjee, E. W. Uffman, S. Gilbertson, P. J. Rosenthal, D. E. Goldberg, *J. Biol. Chem.* **2008**, *283*, 12870–12876.
- [10] B. R. Shenai, P. S. Sijwali, A. Singh, P. J. Rosenthal, *J. Biol. Chem.* **2000**, *275*, 29000–29010.
- [11] A. Singh, P. J. Rosenthal, *J. Biol. Chem.* **2004**, *279*, 35236–35241.
- [12] P. S. Sijwali, B. R. Shenai, J. Gut, A. Singh, P. J. Rosenthal, *Biochem. J.* **2001**, *360*, 481–489.
- [13] C. R. Caffrey, E. Hansell, K. D. Lucas, L. S. Brinen, A. A. Hernandez, J. Cheng, S. L. Gwaltney II, W. R. Roush, Y.-D. Stierhof, M. Bogyo, D. Steverding, J. H. McKerrow, *Mol. Biochem. Parasitol.* **2001**, *118*, 61–73.
- [14] M.-H. Abdulla, T. O'Brien, Z. B. Mackey, M. Sajid, D. J. Grab, J. H. McKerrow, *PLoS Negl. Trop. Dis.* **2008**, *2*, e298.
- [15] C. R. Caffrey, S. Scory, D. Steverding, *Curr. Drug Targets* **2000**, *1*, 155–162.
- [16] R. Ettari, F. Bova, M. Zappalà, S. Grasso, N. Micale, *Med. Res. Rev.* **2010**, *30*, 136–167.
- [17] F. Lecaille, J. Kaleta, D. Brömme, *Chem. Rev.* **2002**, *102*, 4459–4488.
- [18] M. Zürcher, F. Diederich, *J. Org. Chem.* **2008**, *73*, 4345–4361.
- [19] S. X. Wang, K. C. Pandey, J. R. Somoza, P. S. Sijwali, T. Kortemme, L. S. Brinen, R. J. Fletterick, P. J. Rosenthal, J. H. McKerrow, *Proc. Natl. Acad. Sci. USA* **2006**, *103*, 11503–11508.
- [20] T. Hogg, K. Nagarajan, S. Herzberg, L. Chen, X. Shen, H. Jiang, M. Wecke, C. Blohmke, R. Hilgenfeld, C. L. Schmidt, *J. Biol. Chem.* **2006**, *281*, 25425–25437.
- [21] I. D. Kerr, J. H. Lee, K. C. Pandey, A. Harrison, M. Sajid, P. J. Rosenthal, L. S. Brinen, *J. Med. Chem.* **2009**, *52*, 852–857.
- [22] I. D. Kerr, J. H. Lee, C. J. Farady, R. Marion, M. Rickert, M. Sajid, K. C. Pandey, C. R. Caffrey, J. Legac, E. Hansell, J. H. McKerrow, C. S. Craik, P. J. Rosenthal, L. S. Brinen, *J. Biol. Chem.* **2009**, *284*, 25697–25703.
- [23] I. D. Kerr, P. Wu, R. Marion-Tsakamaki, Z. B. Mackey, L. S. Brinen, *PLoS Neglected. Trop. Dis.* **2010**, *4*, e701.
- [24] A. C. Storer, R. Ménard, *Perspect. Drug Discovery Des.* **1996**, *6*, 33–46.
- [25] F. F. Fleming, L. Yao, P. C. Ravikumar, L. Funk, B. C. Shook, *J. Med. Chem.* **2010**, *53*, 7902–7917.
- [26] S. T. Murphy, H. L. Case, E. Ellsworth, S. Hagen, M. Huband, T. Joannides, C. Limberakis, K. R. Marotti, A. M. Ottolini, M. Rauckhorst, J. Starr, M. Stier, C. Taylor, T. Zhu, A. Blaser, W. A. Denny, G.-L. Lu, J. B. Smail, F. Rivault, *Bioorg. Med. Chem. Lett.* **2007**, *17*, 2150–2155.
- [27] H.-H. Otto, T. Schirmeister, *Chem. Rev.* **1997**, *97*, 133–172.
- [28] J. M. Coterón, D. Catterick, J. Castro, M. J. Chaparro, B. Díaz, E. Fernández, S. Ferrer, F. J. Gamo, M. Gordo, J. Gut, L. de Las Heras, J. Legac, M. Marco, J. Miguel, V. Muñoz, E. Porras, J. C. de la Rosa, J. R. Ruiz, E. Sandoval, P. Ventosa, P. J. Rosenthal, J. M. Fiandor, *J. Med. Chem.* **2010**, *53*, 6129–6152.
- [29] R. M. Oballa, J.-F. Truchon, C. I. Bayly, N. Chaurat, S. Day, S. Crane, C. Berthelette, *Bioorg. Med. Chem. Lett.* **2007**, *17*, 998–1002.
- [30] P. R. Gerber, K. Müller, *J. Comput.-Aided Mol. Des.* **1995**, *9*, 251–268.
- [31] CCDC 793262–793264 contain the supplementary crystallographic data for this paper. These data can be obtained free of charge from The Crystallographic Data Centre via www.ccdc.cam.ac.uk/data_request/cif.

- [32] A. Breuning, B. Degel, F. Schulz, C. Büchold, M. Stempka, U. Machon, S. Heppner, C. Gelhaus, M. Leippe, M. Leyh, C. Kisker, J. Rath, A. Stich, J. Gut, P. J. Rosenthal, C. Schmuck, T. Schirmeister, *J. Med. Chem.* **2010**, *53*, 1951–1963.
- [33] F. Schulz, C. Gelhaus, B. Degel, R. Vicik, S. Heppner, A. Breuning, M. Leippe, J. Gut, P. J. Rosenthal, T. Schirmeister, *ChemMedChem* **2007**, *2*, 1214–1224.
- [34] M. Dixon, *Biochem. J.* **1972**, *129*, 197–202.
- [35] J. D. A. Tyndall, T. Nall, D. P. Fairlie, *Chem. Rev.* **2005**, *105*, 973–999.

Received: October 14, 2010

Published online on November 25, 2010
